International Journal of Biological Macromolecules 221 (2022) 784–795

Contents lists available at ScienceDirect

International Journal of Biological Macromolecules

journal homepage: www.elsevier.com/locate/ijbiomac

Dysmyelination and glycolipid interference caused by phenylalanine in phenylketonuria

Valeria Rondelli [a,*], Alexandros Koutsioubas [b], Emanuela Di Cola [a,c], Giovanna Fragneto [d], I. Grillo [d], Elena Del Favero [a], Laura Colombo [e], Laura Cantù [a], Paola Brocca [a,1], Mario Salmona [e,*,1]

[a] Department of Medical Biotechnology and Translational Medicine, Università degli Studi di Milano, Italy
[b] Jülich Centre for Neutron Science (JCNS) at Heinz Maier-Leibnitz Zentrum (MLZ), Forschungszentrum Jülich GmbH, Lichtenbergstrasse 1, 85748 Garching, Germany
[c] SAS-analysis, Saint Egreve, France
[d] Institut Laue-Langevin, 71 Avenue des Martyrs, BP 156, Grenoble Cedex 38000, France
[e] Department of Molecular Biochemistry and Pharmacology, Istituto di Ricerche Farmacologiche Mario Negri IRCCS, Milano, Italy

ARTICLE INFO

Keywords:
GM1
Amyloidogenic fibres
X-ray
Neutron
MLV

ABSTRACT

Phenylketonuria (PKU) is a metabolic disorder connected to an excess of phenylalanine (Phe) in the blood and tissues, with neurological consequences. The disease's molecular bases seem to be related to the accumulation of Phe at the cell membrane surface. Radiological outcomes in the brain demonstrate decreased water diffusivity in white matter, involving axon dysmyelination of not yet understood origin. We used a biophysical approach and model membranes to extend our knowledge of Phe–membrane interaction by clarifying Phe's propensity to affect membrane structure and dynamics based on lipid composition, with emphasis on modulating cholesterol and glycolipid components to mimic raft domains and myelin sheath membranes. Phe showed affinity for the investigated membrane mimics, mainly affecting the Phe-facing membrane leaflet. The surfaces of our neuronal membrane raft mimics were strong anchoring sites for Phe, showing rigidifying effects. From a therapeutic perspective, we further investigated the role of doxycycline, known to disturb Phe packing, unveiling its action as a competitor in Phe interactions with the membrane, suggesting its potential for treatment in the early stages of PKU. Our results suggest how Phe accumulation in extracellular fluids can impede normal growth of myelin sheaths by interfering with membrane slipping and by remodulating free water and myelin-associated water contents.

1. Introduction

The accumulation, fibrillation, and interactions of biomolecules, including proteins and single amino acids, of cells and tissues of different origins are seen in several pathologies [1–4]. Phenylketonuria (PKU, OMIM 261600) is one of the most common inherited metabolic disorders (1:10,000 births), and its onset and progression are connected to an excess concentration of phenylalanine (Phe) in blood and tissues, originating from the impairment of phenylalanine hydroxylase (PAH) enzymatic activity and subsequent incapacity to convert Phe to tyrosine [5,6].

More than 500 different mutations in the PAH gene have been reported, and no specific genotype/phenotype correlation has been found. If not treated, plasma levels of Phe can be high enough to be poorly tolerated (360–600 μmol/L) or even toxic (>600 μmol/L). In the 1950s, it was demonstrated that high blood levels of Phe were the basis for neuropsychological deficits [7], and PKU was soon included in newborn screening. Current adjuvant treatments are based on different hypotheses about the disease mechanism, aiming either to dampen metabolite imbalances by dietary restrictions and other amino acid integration or to stimulate protein synthesis and neurotransmission [8]. Nonetheless, the molecular basis of the disease is still largely unknown, and dietary treatment criteria during aging are under debate [9]. Indeed, there is evidence that this pathology may be reversed with adherence to a strict low-Phe diet [10,11].

A paradigm for interpreting the etiopathology of PKU was proposed

* Corresponding authors.
E-mail addresses: valeria.rondelli@unimi.it (V. Rondelli), mario.salmona@marionegri.it (M. Salmona).
[1] The last two authors contributed equally to this manuscript.

https://doi.org/10.1016/j.ijbiomac.2022.09.062
Received 21 October 2021; Received in revised form 7 September 2022; Accepted 7 September 2022
Available online 12 September 2022

by Adler-Abramovich and coworkers [12], who indicated amyloid-like assemblies in the brains for the first time in transgenic mouse models and patients with PKU. The co-localisation of the typical hallmarks of amyloid-type structures and Phe was used as an indication that the self-assembled structures of the excess Phe could accumulate in the brain and potentially cause neurological illness. Although numerous studies have shown a relationship between high plasma Phe concentration and intellectual impairment, it is not yet clear whether the broader Phe fluctuations in PKU affect the brain by a direct interaction with brain tissues [13].

Major radiological PKU outcomes are obtained by diffusion-weighted NMR imaging, denoting a well-established hyperintensity of several white matter (WM) regions in PKU patients, due to a diminished water diffusion coefficient associated with restricted mobility [14,15]. Abnormalities are mostly recurrent in the periventricular/occipital area and their severity correlates with the amount of accumulated Phe in the brain and blood [11,16,17]. However, abnormalities are not seen to be associated with a loss of anisotropy of water diffusion, which preserves the normal orientation along the direction parallel to the long axis of axons. Quantitative studies on the diffusivity tensor and on water relaxation abnormalities in PKU patients have been performed [14–16,18,19], disentangling the abnormalities that are associated with changes in myelin sheaths. They showed that the decreased diffusion of water was due to a strongly decreased diffusion along the direction of the tract, while the transverse directions of axons were only mildly changed. This would imply an overall integrity of the axons and their myelin sheaths [20] where, in the two-dimensional layers between the glial cell membranes wrapped up around the axon, the water molecules with restricted dynamics reside. Thus, the hypothesis of axon demyelination being at the origin of the adverse neurological implications of PUK seems to be excluded. Importantly, the same authors demonstrated the combined occurrence of an augmented amount of free water and a clear loss of myelin-bonded water in WM lesions, as well as in apparently non-affected regions (regions not affected by hyperintensities) in PKU patients [20]. These findings indicate dysmyelination as a potential mechanism. The degree of diffusivity restriction was found to be age-correlated in periventricular and occipital areas. From a developmental perspective, it was found that the age-dependent decrease in water mean diffusivity during childhood was significantly augmented in PKU patients, with respect to control groups, in different WM regions, even for early and continuously treated patients [9,21,22].

Assessing the Phe–cell surface structural interaction could provide a clue to understanding the mechanism of PKU, besides boosting our understanding of the molecular mechanisms of antimicrobial nanoconstructs and peptides with membrane interactions [23,24]. A study by Do et al. [25] revealed that Phe can aggregate into multiple layers of four zwitterion Phe monomers: at natural pH, monomers form a hydrophilic core made up of the charged termini and expose hydrophobic aromatic side chains, which have been proposed as the linkage for membrane attachment. Interaction with lipid membranes can affect the spatial disposition of amino acids in peptides, resulting in modification of the peptide tertiary structure for their non-interacting counterpart [26,27]. The extent and effect of Phe interaction with membrane lipids have not been widely explored, but Phe shows a propensity for hydrophobic surfaces, and fibrillation may be tuned by lipid charge and pH [28–31]. Phe was also recently shown to increase membrane permeability [32].

Glycosphingolipids, and among them gangliosides, a particular glycosphingolipid class bearing sialic acids on their polar portions, are abundant in the nervous system, and in particular in the neurons, of all animal species [33]. They are involved in cell physiological processes, including differentiation, memory control, cell signalling, neuronal protection, neuronal recovery and apoptosis, being as well associated with functional plasticity of the brain [34]. Notably, glycosphingolipids play a major role in cell–cell adhesion by carbohydrate–carbohydrate interactions among facing membranes [35,36]. Several studies have suggested and proven their role in promoting interactions among facing extracellular surfaces of myelin, promoting dehydration during myelin sheath formation, signal transmission throughout the sheath, and thus facilitating myelin-axonal communication [37–39], stressing the primary role of the exposed galactose [40].

Among gangliosides, GM1, known to be involved in synaptic signalling [41–44] and bearing a galactose as the last most exposed sugar in the headgroup, is found in membrane rafts, together with cholesterol [45–48]. Several nervous system diseases, including most of the neurodegenerative diseases and major forms of dementia, are connected to alterations in sphingolipids metabolism alterations [49–51] and numerous studies involving exogenous addition of ganglioside mixtures or GM1 to cultured neurons indicate that changes of membrane ganglioside content and pattern alter brain responses to signals from the surrounding environment.

Further, amino acid−carbohydrate interactions have been widely studied, highlighting the role played by protein–carbohydrate interactions in biological system functionality and in diseases, and it has been found that specific carbohydrate C−H bonds interact preferentially with aromatic residues, such as the one provided by Phe [52]. In this landscape, the effects of Phe on different membrane domains were investigated to delineate their association with membrane composition, with a dedicated interest in neuronal membrane rafts and myelin sheaths. Of particular interest, the affinity of Phe for various interfaces has been tested in different model membranes containing phospholipids, cholesterol, and GM1 ganglioside [47,48]. The different lipid mixtures used are intended as mimics of membrane segments of different structures, fluidity, and surface properties, thus offering diverse interaction platforms for the incoming Phe, with or without galactose exposure on their external surfaces.

In the present study, the biophysical properties of model membranes in the absence and presence of Phe were studied using combinations of Langmuir isotherms, differential scanning calorimetry, X-ray and neutron small-angle scattering, and neutron reflectometry. Additionally, since we previously demonstrated that mixing Phe aggregates with doxycycline reduced the toxicity of Phe aggregates [53], we conducted neutron reflectometry experiments to clarify the drug's action on the molecular scale. Blood–brain barrier passage is essential in this context, and that of doxycycline has been confirmed in patients with Creutzfeldt-Jakob disease [54]. This property of doxycycline enhances the importance of our studies, opening up a new perspective for the use of the drug in treatment in the early stages of PKU.

2. Results and discussion

We employed different techniques to investigate the structural effects of Phe on different lipid membranes and the extent of its interaction with hydrophobic and hydrophilic membrane segments. The different techniques used in this study call for various measuring conditions and amounts and total concentrations of material. Thus, we prepared and used membranes and Phe in different absolute concentrations, always keeping the lipid:Phe molar ratio in the range of few Phe monomers per lipid.

2.1. Langmuir isothermal experiments: Phe intercalation in lipid monolayers

We studied the lateral packing behaviour of different phospholipid-based lipid mixture monolayers at the air interface with water and over aqueous subphases containing Phe at two concentrations. The phospholipid was the commonly used di-palmitoyl-phosphatidyl-choline (DPPC). The following lipid mixtures were used: 1) pure DPPC, 2) DPPC-cholesterol 10:1.25 mol, 3) DPPC-GM1 ganglioside 10:1 mol, and 4) DPPC-cholesterol-GM1 10:1.25:1 mol. Fig. 1 shows the pressure-area (π-A) isotherms of the mixtures compressed over a subphase of pure water and of two solutions containing Phe: 20 μmol and 2

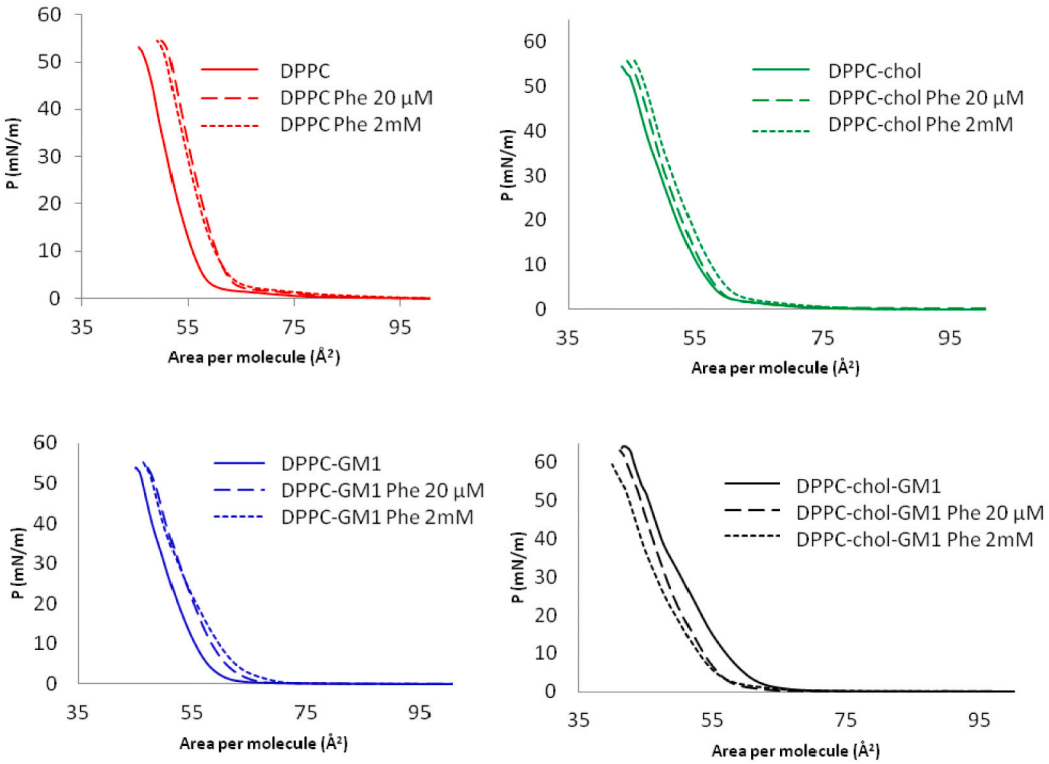

Fig. 1. π-A isotherms recorded at 15 °C for the different lipid mixtures at the air interface with water solutions of Phe at three molar concentrations: 0 (solid line), 2 * 10^{-5} (dashed line), 2 * 10^{-3} (dotted line).

mmol Phe aqueous solutions.

Table 1 reports the minimal areas per molecule (just before monolayer collapse) deducted from the π-A curves: The presence of Phe in the subphase affected the phase behaviour of all the lipid mixtures due to an interaction with lipids, depending on the Phe concentration in the subphase. The higher Phe concentration seemed to hasten the creation of a liquid phase from the gas phase, visible at the higher area-per-lipid values of the monolayers. The effect of Phe (Table 1) on the mono- and bi-component lipid systems increased the mean area per molecule, with a greater effect on the DPPC monolayer, raising the minimal mean area per lipid volume from 46 to 50 Å^2. This effect, already reported [29–31,55], indicates Phe intercalation in the phospholipid heads.

The Phe interplay with the three-component system, the raft mime, was different (Table 1): Phe reduces the mean area per molecule, suggesting either an unfavourable Phe-raft hydrophilic portion interaction affinity, resulting in mutual repulsion, or, more likely [52], a lipid-heads-coordination role of Phe, inducing tighter packing of the ganglioside heads.

In what follows, we present the results of complementary calorimetric and structural investigations, performed to gain additional information.

2.2. *Differential scanning calorimetry: Phe effect on lipid mixture packing*

We investigated the thermotropic behaviour of the model membranes and the effect of Phe presence using differential scanning calorimetry to reveal the energetics of order modifications in membranes caused by Phe. The different lipid mixtures, in the form of large unilamellar vesicles (LUV), were: 1) pure DPPC, 2) DPPC-cholesterol 10:1.25 mol, 3) DPPC-GM1 10:1 mol, and 4) DPPC-cholesterol-GM1 10:1.25:1 mol. Each LUV solution was divided into two halves; the volume of one half was diluted 1:1 with H_2O, while the second half was diluted 1:1 with a 200 mM Phe solution in H_2O. Experiments were performed after 1 h of incubation at 50 °C. Thermograms obtained during the cooling of the sample are reported in Fig. 2, while the temperatures of the main peak associated with the lipid chain melting transition and transition enthalpies are indicated in Table 2.

Calorimetric measurements indicated that Phe interacted with all the investigated membranes. A very small enthalpic effect of Phe was detected, with the largest ΔH change (around 10 %) being shown by the DPPC-GM1 membrane, while the entropic contribution of Phe interaction was evident in the changes of T_m and of C_p (T) peak shape in all the systems. Phe affected the thermotropic behaviour of membranes, stabilising either the fluid or the gel phase, depending on the membrane system it interacted with. On the DPPC and DPPC-cholesterol membranes, Phe stabilised the fluid phase, resulting in a lower lipid chain melting temperature T_m, leaving unchanged the degree of cooperativity of the transition. In the presence of GM1, the enthalpic peak was broader and showed two contributions. Phe caused phase separation, possibly boosting the segregation of GM1-rich domains in membrane that allowed gel-to-fluid transition at higher temperatures [56], with respect to less rich domains characterised by a T_m decrease towards a value similar to that observed for pure DPPC. Additionally, the splitting of the peak may also occur because of an asymmetric behaviour of the two leaflets taking place due to a preferential interaction of Phe with the external membrane leaflet, the source of Phe. The effect was different when cholesterol was present together with GM1. GM1 and cholesterol are known to form a structural couple in membranes [57,58], resulting in the formation of domains ('rafts') where components have lower

Table 1
Minimal area per molecule (±1 Å^2) for the different lipid mixtures at the air interface with pure water and two Phe aqueous solutions.

	In H_2O	In Phe 20 μM	In Phe 2 mM
DPPC	46	51	50
DPPC-chol	44	45	46
DPPC-GM1	46	47	47
DPPC-chol-GM1	43	42	42

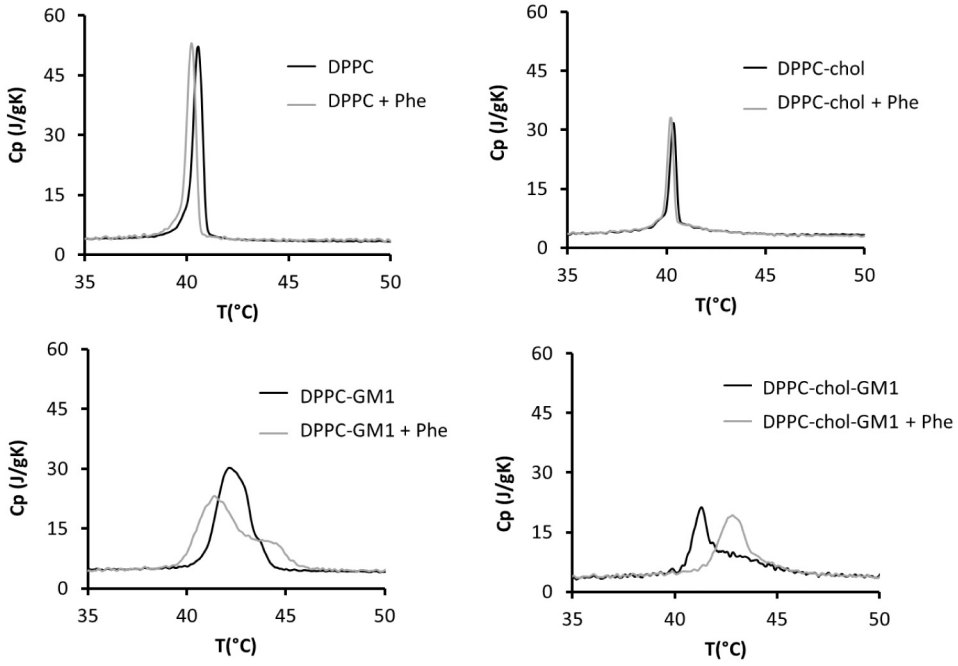

Fig. 2. Thermograms related to cooling scans at 1 °C/3 min, corresponding to the membrane systems (from top to bottom, left to right: DPPC, DPPC-cholesterol 10:1.25 mol, DPPC-GM1 10:1 mol, DPPC-cholesterol-GM1 10:1.25:1 mol) in water (black) or in 100 mM Phe (grey).

Table 2
Temperatures at which the main peaks associated with the lipid chain melting transition reach maximum intensity (T_{max}) and transition enthalpies of the lipid portion of the systems. The last column shows the width of the main peak at half-height (FWHM).

	T_{max} (±0.1 °C)	Enthalpy (±0.2 J/g_{lipid})	FWHM (±0.005)
DPPC	40.6	37.6	0.556
DPPC + Phe	40.2	36.2	0.532
DPPC-chol	40.4	24.2	0.436
DPPC-chol + Phe	40.2	23.4	0.417
DPPC-GM1	42.2	54.1	1.897
DPPC-GM1 + Phe	41.6; 44.7	59.2	2.377 (related to T = 41.6 °C)
DPPC-chol-GM1	41.4; 43.7	37.5	1.199 (related to T = 41.4 °C)
DPPC-chol-GM1 + Phe	43.0	36.6	1.931

mobility. This was reflected in the thermogram that shows two peaks: the sharp one at lower temperatures was comparable in width and melting temperature to that of pure DPPC, and the larger one at higher temperatures was characteristic of a GM1-containing membrane. Phe stabilised the gel phase (increased T_m); as suggested by the area per molecule decrease observed in Langmuir isotherm experiments, and the known affinity between carbohydrates and aromatic residues [39,52], this possibly links to ganglioside heads to promote the formation of ordered domains with lower mobility within the membranes. We observed that Phe impeded the splitting of the enthalpic peak and, on the contrary, promoted a single heat flow event at a higher T_m. This suggests that an outer/inner leaflets co-action occurred, possibly due to a trans-membrane coupling role of the cholesterol-GM1 couple. Each thermogram's main peak was fitted to a Gaussian curve, and the width at half height (FWHM) was extracted (Table 2), the FWHM being related to the lipid degree of cooperativity during the transition. A decrease in the cooperativity of the transition, not accompanied by a modification in enthalpy, suggests that the membranes were not uniform but presented different domains involved in the transition.

2.3. Phe structural interaction with lipid vesicles

Small and wide-angle X-ray scattering (SAXS and WAXS) measurements were performed at the ID02 beamline of the ESRF, Grenoble, France, on LUV with different compositions to investigate the influence of Phe on the membrane structure. SAXS measurements allowed access to the aggregate morphology, while WAXS measurements unveiled any effect of Phe on the lipid chain's local order. The SAXS spectra from the model systems with or without Phe are reported in Fig. 3.

The presence of Phe did not change the bilayer morphology (the bilayer form factor in the q-region around 0.1 $Å^{-1}$) in any of the membrane systems. The amino acid contribution to the scattering signal was evidenced only in the lower q-region of the SAXS spectra, where the technique was sensitive to the vesicular aggregates as a whole, and the effect on the overall dimension depended on the membrane composition. SAXS data were fitted by modelling the vesicles as spheres with a water core and three shells intended as inner leaflet heads, chains, and outer leaflet heads. The comparison of the SAXS profiles of the different membranes in the absence and presence of Phe are reported in the Supplementary Materials, as well as the vesicles' radii (see Table S1). The most evident effect of Phe was on DPPC-cholesterol vesicles, whose radius decreased by 14 % (from the original 44 ± 1 nm to 38 ± 1 nm). This reduction may be due to Phe interacting with the external lipid leaflet. The excess area only in the external membrane portion would reduce the molecules' packing parameter, forcing an increase of the curvature, then favouring the formation of smaller aggregates.

No shift was observed in the WAXS peaks (q-region around 1.5 $Å^{-1}$), corresponding to the typical lipid chain-to-chain distance (data not shown) for all the membranes after interaction with Phe, suggesting that the interaction may possibly be confined to the membranes' external layers.

For further structural studies, small-angle neutron scattering (SANS) investigations were carried out on similar systems, using deuterated lipids to easily detect H-containing molecules (such as Phe) in the target membrane lipid chains.

SANS experiments were performed on the D33 instrument at the Institut Laue-Langevin (ILL), Grenoble, France. Deuterated-chain phospholipids in deuterated water (D_2O) were used to detect Phe across the

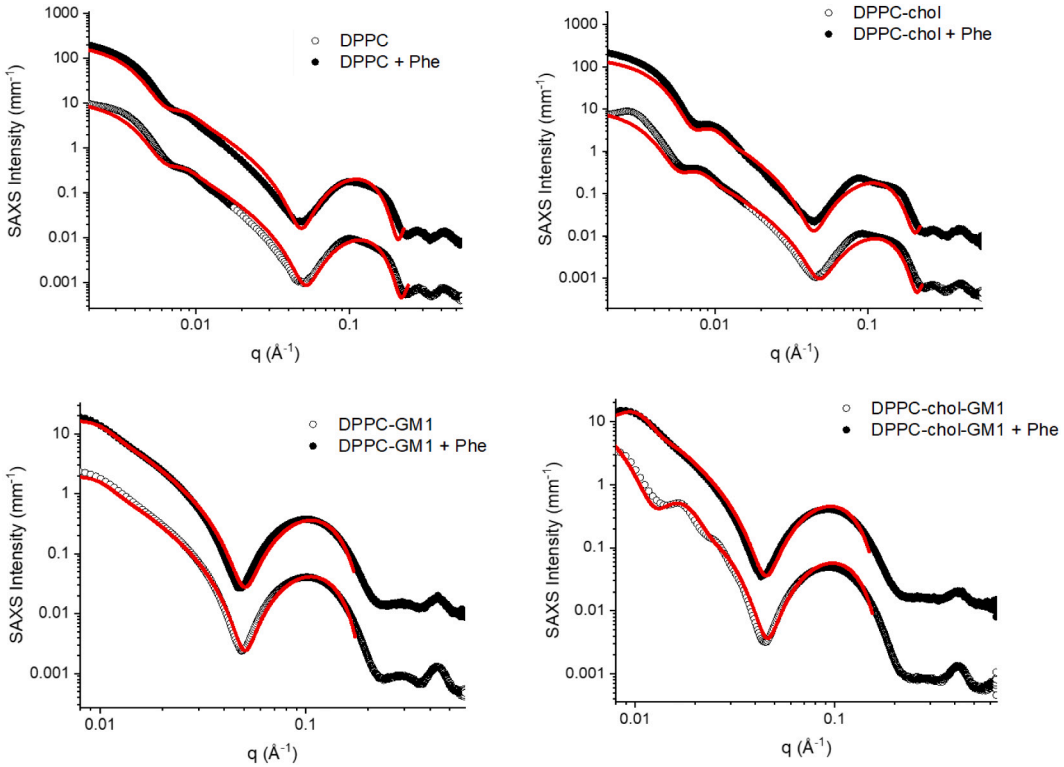

Fig. 3. SAXS spectra of the large unilamellar vesicles (LUVs) interacting (full symbols, intensity ×10) or not (empty symbols) with Phe at room temperature. Red lines indicate the best data fit.

membrane hydrophobic portion. As for calorimetric and SAXS/WAXS investigation, we prepared model membranes in the form of LUVs. Each membrane solution was then divided into two, and one-half was diluted 1:1 with D_2O, while the second half was diluted 1:1 with 200 mM Phe in D_2O.

The data in Fig. 4 were analysed with a similar core-3 shell model as that used to analyse the SAXS data. The scattering length density profiles from the membranes given the data best fit are reported in the Supplementary Materials, Table S2. The membrane layers (q-region around 0.1 Å^{-1}) showed no contrast variation after interaction with Phe, although in some cases Phe—possibly inducing osmotic shock to the LUVs—caused the spontaneous formation of multi-layered structures (peaks in the q-region around 0.1 Å^{-1}), the most evident case shown here being from the DPPC sample.

In what follows, we present a deep investigation of this effect with a dedicated experiment reported in the section on SAXS from raft mimes: 'Mimicking the intracellular diffusion of Phe'.

Phe had no effect after interaction with the raft-like three-component DPPC-cholesterol-GM1 membrane, whereas in the other three systems, there was a small increase in the lipid chain scattering length density—a sign of a slight increase in the lipid chain packing after the interaction.

As evidenced by the SAXS, the whole aggregate sizes and structuring were modified in some cases, as indicated by the low q region spectra. Again, in the DPPC-cholesterol membrane, Phe had a very strong effect, and the vesicles' inner radius was reduced by 18 % (from 38 ± 1 to 32 ± 1 nm). The inner core radius was reduced by 11 % (from 35 ± 1 to 31 ± 1 nm) for the DPPC membranes, by 5 % (from 21 ± 1 to 20 ± 1 nm) for the DPPC-GM1 membranes, and by 8 % (from 26 ± 1 to 24 ± 1 nm) for the DPPC-cholesterol-GM1 membranes after interaction with Phe.

In the very low-q vector region, the data were not consistent with the fitted model. Two aspects may be considered in explaining the observed intensity oscillation: i) a structure factor contribution accounting for inter-vesicle order, being GM1-containing LUVs charged, and ii) the typical mark coming from the occurrence of GM1-rich patches [56] laterally segregated within the membrane [59], highlighted by the high contrast in the membrane made of deuterated lipids in D_2O. Combining the SANS and SAXS results, it is plausible that, since Phe does not dampen the low-q oscillations in SANS spectra, the detection of GM1-rich patches may be at the origin of the observed features, even if DSC indicates that at the molecular level, the lateral distribution of components is affected in GM1-containing membranes after the interaction with Phe. Nonetheless, a unique data interpretation is then not straightforward and would require investigating the systems at lower *q* vector values.

Together, the SANS and SAXS results as a whole suggest that the interaction of Phe with the membrane is limited to the membrane external leaflet. However, the full extent of the interaction of Phe with the membrane surface was not addressed. Therefore, we performed neutron reflectometry (NR) measurements from planar membrane systems.

2.4. Single membrane studies by neutron reflectometry

NR is the technique of choice for studying changes in the transverse structure of membranes in one or more regions due to interactions with external molecules [57,58,60–63]. Measurements were performed using the MARIA reflectometer at the Jülich Centre for Neutron Science (JCNS) at Heinz Maier-Leibnitz Zentrum (MLZ, Garching, Germany) and the D17 reflectometer at the ILL.

After complete characterization of the target membranes, prepared with the same composition as the LUVs studied by calorimetry, SANS, and SAXS, Phe was injected into the measuring cells to a final bulk concentration of 20 μM. The solid support under the membranes made the system rigid, reducing the lateral mobility of the membrane components. Therefore, we performed NR experiments at high temperatures in which the lipid chains were in the fluid phase. Measuring reflectivity again showed whether any interaction had taken place and, if so, the depth of the membranes at which it occurred, since the Phe scattering

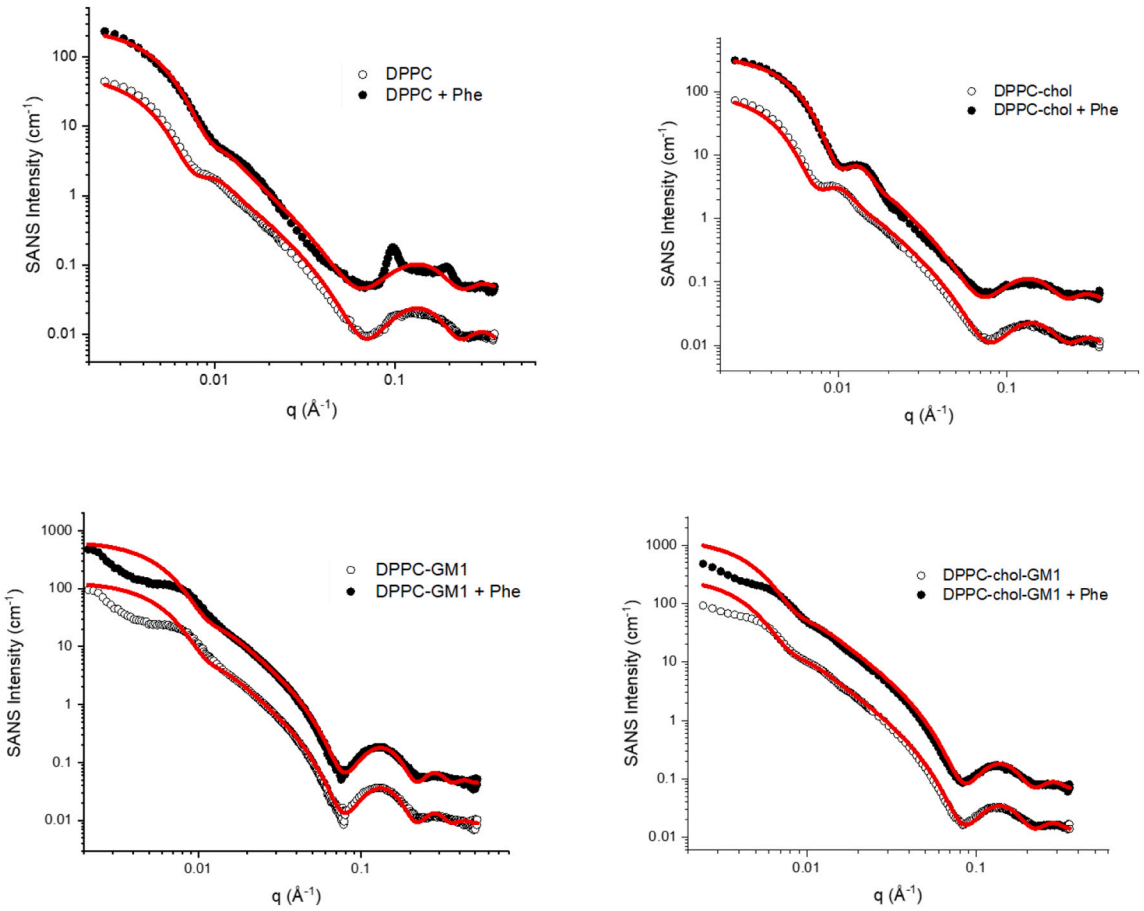

Fig. 4. SANS Spectra of the large unilamellar vesicles (LUVs) investigated in interaction with Phe (full symbols, intensity ×10) or not (empty symbols) in the lipid fluid phase at 50 °C. Red lines indicate the best data fit.

length density (SLD) (2.17 * 10^{-6} Å^{-2}) was different from that of lipid chains (around 7.11 * 10^{-6} Å^{-2}) and head chains (1.75 * 10^{-6} Å^{-2}). Subsequently, water was gently flushed in the measuring cells to study the extent of any Phe–membrane interaction.

Data were analysed by modelling each membrane as composed of four layers, two hydrophilic and two hydrophobic, to account for asymmetry in their hydrophobic tails.

All the spectra with their best fits and the resulting SLD profiles are reported in the Supplementary Materials. As an example (Fig. 5), the spectra for the chain deuterated d_{62}DPPC membrane before and after interaction with Phe and after rinsing are reported with their best fit and the SLD profiles. Fit parameters are summarised in Table 3.

The NR showed that the interaction of Phe with single supported membranes was limited to the external membrane leaflet, and this was evident from the SLD variation after Phe interaction, involving only membrane external leaflet. As the membranes were deposited on rigid substrates, penetration was more complicated than in suspended vesicles, and eventual lipid redistribution after interaction was unfavoured. Nonetheless, the results are consistent with the Langmuir isotherms, SAXS, SANS, and DSC investigations. One of this technique's advantages is that it provides information about the propensity of incoming molecules to interact with the membranes of interest.

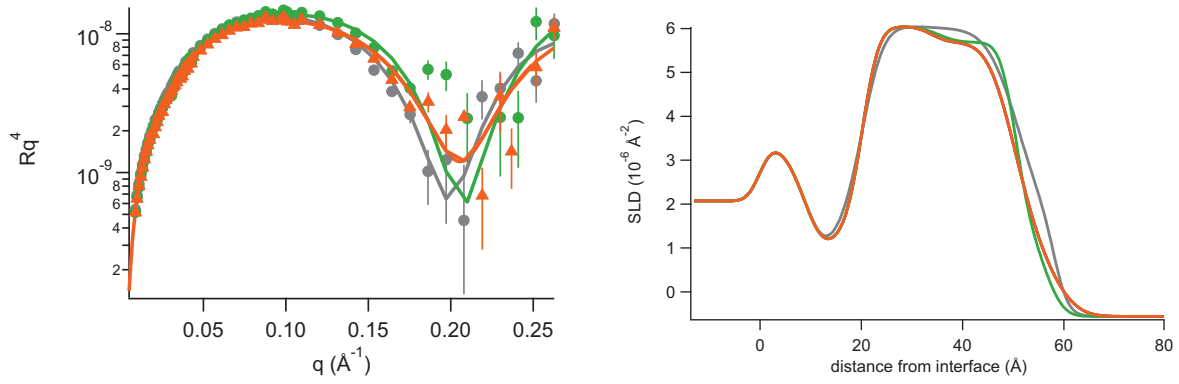

Fig. 5. *Left panel* – Reflectivity spectra of the d_{62}DPPC membrane before (grey) and after (green) interaction with Phe and after flushing with water to remove the excess Phe (orange). Lines indicate the best data fits. *Right panel* – SLD profiles of the membrane, given by the best data fit (same colours). The solvent is H_2O and T 45 °C.

Table 3
Fit parameters of a d_{62}DPPC membrane before and after Phe interaction and after rinsing Phe excess. T: layer thickness (±1 Å); $\rho_l(z)$: average scattering length density of the non-water components of the layer (±0.05 10^{-6} Å^{-2}); W: percent water content of the layer (±3 % in volume); r: roughness between one layer and the adjacent previous one (±2 Å).

	DPPC				DPPC + Phe				DPPC + Phe flushed			
	T	$\rho_l(z)$	W	r	T	$\rho_l(z)$	W	r	T	$\rho_l(z)$	W	r
Water	3				3				3			
Heads in	6	1.75	22	3	6	1.75	22	3	6	1.75	22	3
Chains in	15	7.11	14	3	15	7.11	14	3	14	7.11	14	3
Chains out	16	7.11	14	3	15	6.75	14	3	16	6.75	14	3
Heads out	7	1.75	22	5	6	1.95	22	3	8	1.89	22	4

As expected, there was no deep interaction with the membrane's inner leaflet (the one formed by the lipids directly in contact with the silicon substrate).

Table 4 lists the membrane external layers (distinguished in hydrophilic and hydrophobic) SLD values before and after the interaction with Phe and after rinsing.

Not only Phe presence but also a decrease in the lipid chain packing induced the lowering of the layer scattering length density. Therefore, we focused on SLD relative variation trends.

Both the propensity and the extent of interaction of Phe with membranes depend on the membrane lipid composition, and Phe interaction with the hydrophobic core of the bicomponent membranes was facilitated. NR after membrane flushing indicated that the extent of Phe–membrane interaction also depended on membrane composition. Whereas we observed that the effect (Phe intercalation and/or lipid packing modification) was more evident with the lipid hydrophobic tails, NR also confirmed that the interaction with the hydrophilic part was more robust in the cholesterol-DPPC membrane, as shown by SANS and SAXS, in which a deep modification and leaflet anti-symmetrisation of lipid packing was deduced from LUV size decrease in the presence of Phe.

There was no intercalation of Phe within the raft model membrane, in agreement with what was observed by Langmuir isotherm experiments. The interaction may take place with the exposed glycolipid head portions [39,52] protruding from the membrane surface, which do not give rise to a significant optical layer (30 % in area). This hypothesis was corroborated by the results of the other techniques, indicating that Phe may interact with sugar polar heads, and their coordination may allow aggregation to start towards the extracellular solvent. The dedicated SAXS experiment to clarify this point is reported in the section 'SAXS from raft mimes: mimicking the intracellular diffusion of Phe'.

We advanced single membrane studies by allowing Phe to interact with a floating bilayer. A floating [57,58] d_{62}DPPC membrane system was prepared over a d_{70}DSPC (chain deuterated di-stearoyl-phosphatidyl-choline)-supported bilayer to study the effects of Phe on a membrane decoupled from the solid support, where 3D dynamics is favoured. The system was heated up to 45 °C, above the lipid chain gel-to-fluid transition, and reflectivity was measured. Phe was then injected into the measuring cell (to a final bulk concentration of 20 μM) and after 30 min, reflectivity was measured again. Surprisingly, after the interaction, the effect was the same as if the floating membrane coverage had increased (see SLD in Fig. 6 and fit parameters in Table 5), which may be interpreted by a Phe-induced increase in the membrane rigidity, similarly to what was reported by Nandi and coworkers for the L and *D*-phenylalanine interaction with LAPC vesicles [64].

We hypothesise that before interaction with Phe, the floating fluid membrane presents structural protrusions. This would lift material away from the silicon-supported membrane-proximal layers, which contributed mostly to the reflectivity signal (SLD 7.11 * 10^{-6} Å^{-2}) with respect to the bulk water (H_2O SLD -0.56 * 10^{-6} Å^{-2}, D_2O SLD 6.36 * 10^{-6} Å^{-2}). Thus, the data may be inadequately interpreted as coming from a membrane with low coverage and presenting holes. Instead, the total amount of lipids was larger than what was visible from the reflected neutrons. In other words, if the protrusions were long and dispersed enough, they would not significantly affect the mass detectable by reflectivity. Our interpretation is that when Phe was injected, it reached the membrane and intercalated into the lipid heads, decreasing the membrane's out-of-plane flexibility. Any protrusions were then dampened, and the high convex local curvatures were no longer allowed because of the increased membrane rigidity, and the membrane became flatter. As a result, there was an apparent increase in membrane coverage, which proves Phe action.

To investigate more deeply the role of Phe in the surface interaction with model rafts (DPPC-cholesterol-GM1), we designed a SAXS experiment to mimic the intracellular diffusion of Phe and its effect on facing cell surfaces. We put a raft mimic solution (LUVs) and a Phe solution in contact with a horizontal capillary, and we measured the effect of the diffusion of one solution into the other over time. SAXS measurements were collected at room temperature for 12 h in different positions along the length of the capillary. The results are illustrated in Fig. 7 and indicate that mixing was fast and that Phe induced the formation of multilamellar vesicles (MLV) from the initial unilamellar structures. The formation of multilamellar structures started from the Phe-richer sample portions and was due (data not shown) to an osmotic shock sensed by the membranes at a temperature lower than the membrane transition temperature. This experiment corroborates the hypothesis that Phe links exposed carbohydrates by reducing their electrostatic repulsion, thus favouring the formation of quite close multilamellar structures. The membrane-to-membrane distance in the multilamellar vesicles was seen to vary, reducing to a final value of 9 nm. At low Phe content, in the vesicle-rich portion of the capillary and at the earliest delay times (left column/top spectra in Fig. 7), the initial MLV membrane-to-membrane distance was 11 nm. After a few hours (the total experimental time was 12 h), during which Phe diffused and concentrated homogeneously

Table 4
Membrane external hydrophilic and hydrophobic SLDs (±0.05 10^{-6} Å^{-2}) values before and after the interaction with Phe and after rinsing, as obtained by neutron reflectometry data analysis.

	Before Phe interaction		After Phe interaction		After flushing	
	Hydrophobic	Hydrophilic	Hydrophobic	Hydrophilic	Hydrophobic	Hydrophilic
DPPC	7.11	1.75	6.75	1.95	6.75	1.89
DPPC-chol	6.57	1.75	5.58	1.9	5.59	1.88
DPPC-GM1	6.54	1.84	5.14	1.88	5.21	1.84
DPPC-chol-GM1	4.97	1.78	4.97	1.78	4.97	1.78

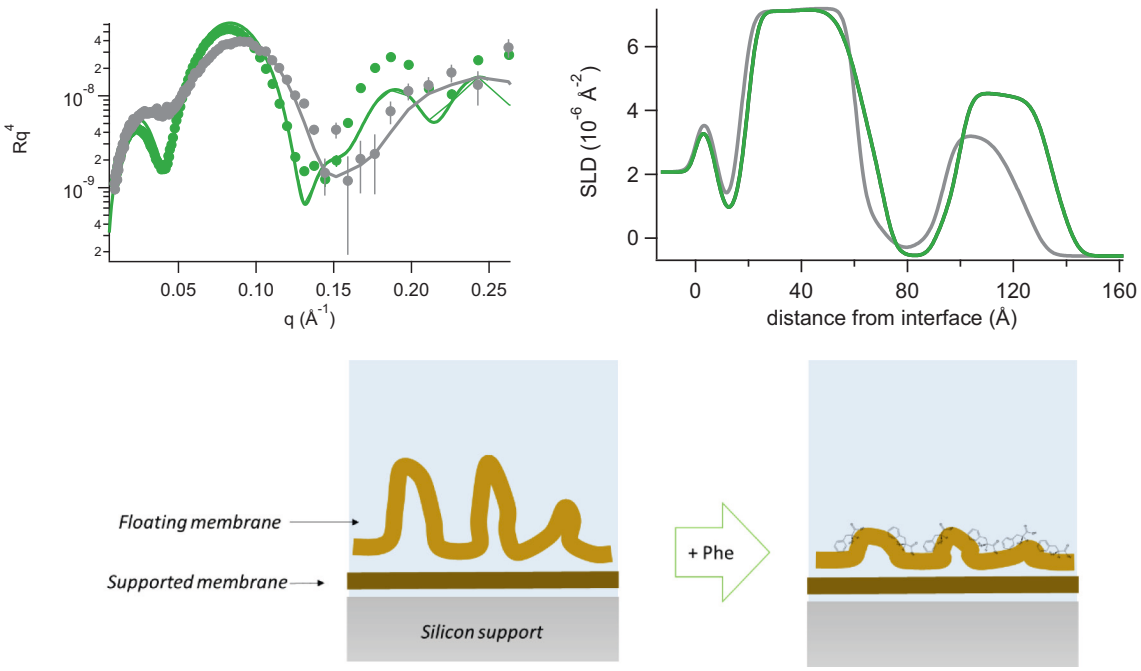

Fig. 6. Upper panel: Neutron reflectometry spectra (left) and scattering length density profiles (right) of the d_{62}DPPC floating membrane before (grey) and after (green) interaction with Phe. The solvent is H_2O, at 45 °C. Lower panel: a sketch of data interpretation.

Table 5
Fit parameters of the d_{70}DSPC/d_{62}DPPC double membrane system before and after Phe interaction. T: layer thickness (±1 Å); $\rho_l(z)$: average scattering length density of the non-water components of the layer (±0.05 10^{-6} Å^{-2}); W: water content of the layer (±3 % in volume); r: roughness between one layer and the previous adjacent one (±2 Å). Measurements were performed at 45 °C.

		d_{70}DSPC/d_{62}DPPC				d_{70}DSPC/d_{62}DPPC + Phe			
		T	$\rho_l(z)$	W	r	T	$\rho_l(z)$	W	r
Supported d_{70} DSPC	Heads in	9	1.75	15	3	9	1.75	15	3
	Chains in	21	7.9	10	5	21	7.9	10	5
	Chains out	21	7.9	9	3	21	7.9	9	3
	Heads out	9	1.75	20	4	9	1.75	20	4
	Water	16			3	20			3
Floating d_{62} DPPC	Heads in	8	1.75	60	7	8	1.75	40	3
	Chains in	13	7	50	6	18	7	32	3
	Chains out	13	7	50	3	15	7	35	4
	Heads out	9	1.75	60	7	8	1.75	40	5

along the capillary, the distance turned to 9 nm, the same as for the whole sample. Considering that a reduction in membrane thickness was not supported by our SANS and SAXS data, the shorter membrane-to-membrane distance was probably due to a reduction in the thickness of the intramembrane water layer. One hypothesis is that for large enough amounts of Phe confined in the water interlayer, stacks/fibres may form, which coordinate the membranes, reducing their reciprocal distance.

Lastly, complementary techniques that have been used in diverse model systems were applied to deepen our understanding of the Phe-membrane interaction, each of them highlighting a peculiar aspect of the amino acid interplay within the different domains. With mono- and bi-component membrane domain mimics, the amino acid was shown to penetrate the external membrane layer, imposing lipid rearrangement and disordering. However, Phe interaction with raft mimes significantly enriched in cholesterol and glycolipids (GM1) was shown to be different. Experiments on Langmuir monolayers showed that when Phe was present in the bulk water, the monolayer mean area per molecule was reduced, suggesting an unfavourable Phe penetration in the raft but a lipid-heads-coordination role. DSC showed that Phe stabilised the gel phase (increased T_m) of raft-like vesicles, promoting the formation of domains within the membranes where lipid components were less mobile. SAXS and SANS experiments indicated that the effect of Phe on the whole aggregate size and lipid packing in the raft mimes was negligible, whereas it was clearly visible in DPPC-cholesterol systems. NR indicated that, although Phe affected the composition and density of the external membrane leaflet of mono- and bi-component target membranes, it had no effect on the raft membrane integrity; not even penetration of the amino acid was detected in such a system. The hypothesis drawn from our experiments is that Phe interaction with the raft mime membrane is limited to the external atoms possibly driven by GM1 protruding polar heads as interaction sites that, in the presence of cholesterol, would have a lateral/transversal arrangement able to anchor Phe. The ad-hoc designed SAXS experiment, mimicking Phe diffusion in the extracellular space, showed that once Phe was anchored to the raft mime surface, it was able to coordinate neighbouring membranes, reducing their reciprocal distance and possibly inter-membrane gluing spots. This is understood by assuming Phe's capability to interact with the exposed carbohydrates [52]. This finding opens up the potential for a strong disturbing action of brain-accumulated Phe when axon myelination occurs. In fact, any growing mechanism allowing myelin sheath expansion to build axon envelops requires membranes to be free to slip over each other. Moreover, carbohydrate–carbohydrate interactions among the facing membrane layer are suggested to provide the dehydration of the extracellular interlayer needed to compact the myelin sheaths [36]. Phe interaction would impair the slipping process and compete with the mutual interaction of carbohydrates, and this interfering action could mediate the formation of vacuoles among the otherwise compacting myelin membranes, right during their formation. Phe effect could be diminished on ended myelinisation stages. From a developmental point of view, we may speculate that Phe excess can be quite effective in early life aging but may be less relevant when WM development has concluded. As clearly indicated by other authors [18]

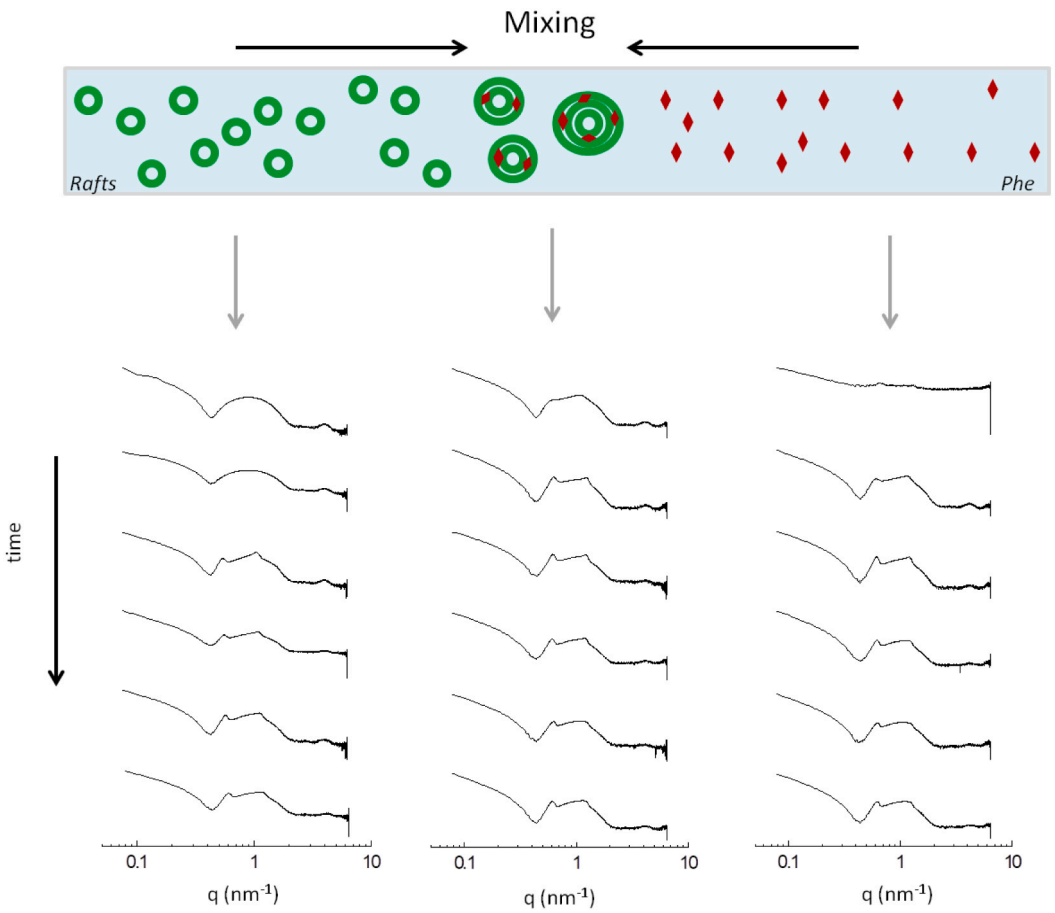

Fig. 7. Experimental simulation of Phe diffusion in intracellular space. The sketch depicts an experiment consisting of directly putting the raft and Phe solutions in contact in the capillary and measuring the structural evolution of the mixing system in different positions along the capillary.

the sole vacuolisation may account for the WM abnormalities observed by MRI in PKU patients, that are the increased amount of free water contributions, due to the less strict confinement of water among layers, as well as the restricted water diffusivity on the longitudinal axon direction, due to increased longitudinal barriers. Moreover, more swollen myelin sheaths, due to impeded slipping, would determine the observed strong decrease of myelin-bonded water, also measured in the WM areas of PKU patients [65,66]. In this view, the observed reversibility of dysmyelination upon dietary restrictions may be partially sustained by the lifelong turnover of myelin sheath components, even after cellular development has ended [67].

Beyond the above-described structural effects, the involvement of GM1 glycolipids in Phe dysmyelination action may be of relevance concerning the neuropsychological deficits in PKU patients, corroborated by the known neurofunctional role of glycosphingolipids in cell membranes [34–38] as well as in myelin membranes [68] and on their formation [37,38].

2.5. Neutron reflectometry from supported membranes: Doxycycline's competitive role

We recently demonstrated that mixing Phe aggregates with doxycycline reduced the toxicity of Phe aggregates [53], paving the way for a putative role of this drug in the treatment of PKU. Drug passage across the blood–brain barrier is essential in treatment, and doxycycline's ability to cross the barrier in patients with Creutzfeldt-Jakob disease was recently confirmed [54]. We therefore investigated the nature of doxycycline action in model membrane-based experiments to help clarify the mechanism of how the drug prevents toxicity.

We designed complementary experiments to investigate the effect of doxycycline both after the Phe–membrane interaction and concomitantly with Phe incubation with the target membrane. Before our investigation, we tested whether incubating a very small amount of doxycycline (1 μM) on a d_{62}DPPC membrane visibly affected the membrane structure. The test indicated that membrane penetration occurs and affects its structure along all cross-sections (see Supplementary Materials). Thus, some interaction of doxycycline with the target membrane was, in principle, recognised.

As a first test, doxycycline was injected at a 1 μM concentration into the measuring cell only after d_{62}DPPC membrane-Phe interaction and flushing of excess amino acid. In this experiment, we intended to investigate the propensity of doxycycline to remove Phe molecules linked to the membrane a posteriori. However, doxycycline was attracted to the membrane, and the interaction occurred without 'safe' removal of Phe.

We repeated this experiment on membranes with different compositions (see Supplementary Materials), with the same results. Therefore, we deposited and characterised a new d_{62}DPPC membrane. We injected Phe premixed with a small amount of doxycycline (Phe 20 μmol, doxycycline 1 μmol to the Phe:doxycycline 1:0.05 mol ratio) into the measuring cell.

In the presence of doxycycline, Phe interaction with the membrane was not favoured (Fig. 8 and Table 6). Moreover, the interaction was limited to the external hydrophilic portion of the membrane, as if Phe molecules were more attracted to and recruited from doxycycline than from the membrane.

In agreement with our previous results [46], these findings strengthen the hypothesis that doxycycline acts as an antagonist in Phe

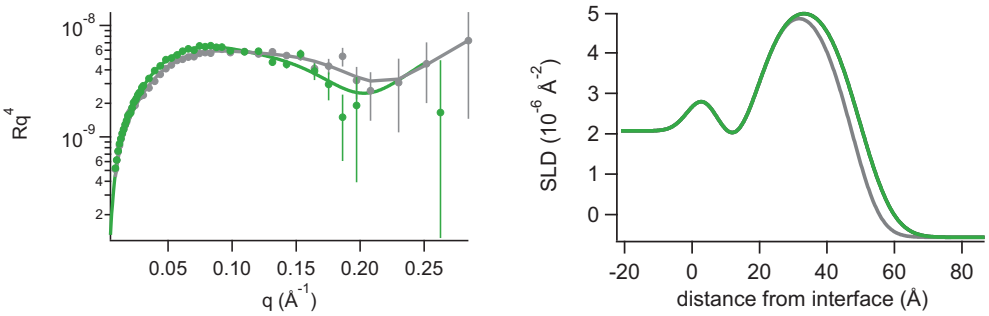

Fig. 8. *Left panel* – Reflectivity spectra of the d_{62}DPPC membrane before (grey) and after (green) interaction with Phe + doxycycline. Lines indicate the best data fits. *Right panel*: SLD profile of the membrane given by the best data fits (same colours). The solvent is H_2O, at 45 °C.

Table 6
Fit parameters of a d_{62}DPPC membrane before and after interaction with Phe: doxycycline 1:0.05 mol. T: layer thickness (±1 Å); $\rho_l(z)$: average scattering length density of the non-water components of the layer (±0.05 10^{-6} Å^{-2}); W: percent water content of the layer (±3 % in volume); r: roughness between one layer and the adjacent previous one (±2 Å).

	DPPC				DPPC + (Phe/doxycycline)			
	T	$\rho_l(z)$	W	r	T	$\rho_l(z)$	W	r
Heads in	9	1.75	35	4	9	1.75	35	4
Chains in	13	7.11	22	4	14	7.11	22	4
Chains out	13	7.11	22	4	14	7.11	22	5
Heads out	6	1.75	35	4	7	1.77	35	6

interaction with membranes, and may be useful to prevent PKU disease and treat it during the early stages.

3. Conclusion

Here, we present a study of the mechanisms of interaction of Phe with model membranes through a variety of techniques to extend our knowledge of specific Phe–membrane interactions and illustrate Phe propensity to couple with different membrane portions. We used various lipid mixtures and different configurations (monolayers, dispersed vesicles, and single supported membranes) to investigate diverse aspects of the amino acid–membrane interaction. The applied techniques highlight the diverse details of the different aspects of the amino acid interaction with the membrane and the role of carbohydrates in the Phe–membrane interaction.

The amino acid was shown to penetrate the external membrane layer of mono- and bi-component systems, imposing lipid rearrangements associated with a general decrease in the melting temperature. However, Phe interaction with the lipid bilayer mime of neuronal raft and myelin sheath membranes (phospholipid, cholesterol, and galactose exposing glycolipids) was shown to be limited to the most external portion of the membrane, populated by the protruding GM1 polar heads. The presence of cholesterol, the GM1 pairing molecule in rafts [45–48], possibly has an effect on GM1 lateral/transversal arrangement for the better anchoring of Phe. This was manifested in different experiments, including in the stabilised gel order (melting temperature increase associated with a lower mobility) and the reduced membrane phase separation degree, visible in the DSC thermographs as well as assessed at the nanoscale by NR experiments.

Neutron reflectometry measurements on floating membrane systems showed that Phe limited the local bending ability of phospholipid membranes, and Langmuir isotherms and calorimetry experiments on this raft model system show that Phe stabilises the membrane gel phases with respect to fluid ones, thus decreasing membrane component mobility. A SAXS experiment designed to mimic the intercellular diffusion of Phe supported the hypothesis that, when interacting with raft-like membranes, Phe coordinates the adjacent layers, reducing their reciprocal distance. Overall, our results indicate that rafts are a putative robust anchoring site for Phe on the outer membrane layer of cells.

Besides boosting the understanding of the molecular mechanisms of the interactions of antimicrobial nanoconstructs and peptides with membranes, these findings may represent an important step forward in today's understanding of PKU, one of the most common inherited metabolic disorders, whose progression is connected with an excess of Phe in blood and tissues. In particular, Phe accumulation in the white matter of the brain is known to produce structural and dynamic abnormalities detected by magnetic resonance imaging in different areas. Our results suggest that Phe interaction with myelin membranes may account for the observed alterations by impeding normal wrapping and promoting vacuolisation by affecting the interaction among glycosphingolipids. Swollen myelin sheaths and vacuole formation are the main suspected processes that explain the restricted water diffusivity and diminished myelin-bonded water in favour of augmented free water measured in PKU patients [18,20,68]. This, together with the finding of a Phe–GM1 headgroup interaction involved in structural outcomes, opens up new perspectives for the comprehension of the molecular mechanisms of the disease, with implications on the neurological aspect and on treatment, for which data are still lacking. In fact, our findings suggest that aging places a limit on the success of dietary treatment when white matter development becomes less important.

Having depicted a possible mechanism for the effect of Phe accumulation on myelination, we exploited the knowledge gained from the research and treatment of amyloidogenic diseases to test a possible Phe antagonist drug. In 2001, we first described the anti-amyloidogenic activity of tetracyclines [69]. Since then, many independent studies have confirmed this, and clinical trials have been carried out on different pathologies secondary to amyloid formation. For instance, at present, 10 clinical trials are listed on the ClinicalTrials.gov website referring to the use of doxycycline for the treatment of different forms of amyloidosis [70,71]. To gain further insight into doxycycline activity, we performed neutron reflectometry experiments that showed that the drug interfered with Phe packing, reducing its toxicity [53]. Doxycycline could not detach Phe from membranes once the interaction had taken place, but it could impede Phe interaction with membranes, acting as an antagonist. Our results open new perspectives for the potential use of doxycycline to prevent PKU disease and treat it during the early stages.

Funding

This research was partly funded by the 'Medical Biotechnology and Translational Medicine Department' of the 'Università degli Studi di Milano', grant number 'PSR2018', to V.R.

CRediT authorship contribution statement

Conceptualisation, V.R., M.S., L.Co., L.Ca., P.B., E.DF.; Langmuir

Films: V.R.; Calorimetry: V.R.; X-Ray: V.R., L.Ca., P.B., E.DF.; Small angle neutron scattering: I.G., L.Ca., V.R., P.B., E.DF., E.DC.; Neutron reflectometry: V.R., L.Ca., P.B., E.DC., A.K., G.F.; Data Analysis, V.R., P. B.; Writing – Original Draft Preparation, V.R., P.B., M.S.; Writing – Review & Editing, all authors.

Declaration of competing interest

The authors declare that they have no known competing financial interests or personal relationships that could have appeared to influence the work reported in this paper.

Availability of data and materials

The SANS and reflectometry datasets generated at the Institute Laue-Langevin (ILL, Grenoble, France) and analysed during the current study are available in the ILL repository (https://doi.org/10.5291/ILL-DATA.8-02-799; https://doi.org/10.5291/ILL-DATA.8-03-893). The other datasets used and analysed during the current study are available from the corresponding author on reasonable request.

Acknowledgements

The authors thank the instrument teams of MARIA, Jülich Centre for Neutron Science (JCNS) at Heinz Maier-Leibnitz Zentrum (MLZ, Garching, Germany), of D17 and D33 at the Institut Laue-Langevin (ILL, Grenoble, France), and ID02 beamline at the European Synchrotron Radiation Facility (ESRF, Grenoble, France) for support and the facilities for allocation of beamtime.

The authors also thank ILL for the use of PSCM facilities and for technical support.

Appendix A. Supplementary data

Supplementary data to this article can be found online at https://doi.org/10.1016/j.ijbiomac.2022.09.062.

References

[1] P. Chakraborty, E. Gazit, Amino acid based self-assembled nanostructures: complex structures from remarkably simple building blocks, ChemNanoMat 4 (8) (2018) 730–740.
[2] S. Bera, S. Mondal, S. Rencus-Lazar, E. Gazit, Organization of amino acids into layered supramolecular secondary structures, Acc. Chem. Res. 51 (9) (2018) 2187–2197.
[3] C.A. Ross, M.A. Poirier, Protein aggregation and neurodegenerative disease, Nat. Med. 10 (2004) S10.
[4] F. Chiti, C.M. Dobson, Protein misfolding, functional amyloid, and human disease, Annu. Rev. Biochem. 75 (2006) 333.
[5] J.J. Mitchell, Y.J. Trakadis, C.R. Scriver, Phenylalanine hydroxylase deficiency, Genet. Med. 13 (8) (2011) 697.
[6] N. Blau, F.J. van Spronsen, H.L. Levy, Phenylketonuria, Lancet 376 (2010) 1417.
[7] S. Yano, K. Moseley, T. Bottiglieri, E. Arning, C. Azen, Maternal phenylketonuria international collaborative study revisited: evaluation of maternal nutritional risk factors besides phenylalanine for fetal congenital heart defects, J. Inherit. Metab. Dis. 37 (2014) 39.
[8] K.M. Camp, Phenylketonuria scientific review conference: state of the science and future research needs, Mol. Genet. Metab. 112 (2014) 87.
[9] E. Wesonga, J.S. Shimony, J. Rutlin, D.K. Grange, D.A. White, Relationship between age and white matter integrity in children with phenylketonuria, Mol. Genet.Metab.Rep. 7 (2016) 45–49.
[10] U. Bick, K. Ullrich, U. Stober, H. Moller, G. Schuierer, A.C. Ludoph, C. Oberwittler, J. Weglage, U. Wendel, White matter abnormalities in patients with treated hyperphenylalaninaemia: magnetic resonance relaxometry and proton spectroscopy findings, Eur. J. Pediatr. 152 (1993) 1012–1020.
[11] A. Cleary, J.H. Walter, J.E. Wraith, J.P. Jenkins, S.M. Alani, K. Tyler, D. Whittle, Magnetic resonance imaging of the brain in phenylketonuria, Lancet 344 (1994) 87–90.
[12] L. Adler-Abramovich, L. Vaks, O. Carny, D. Trudler, A. Magno, A. Caflisch, D. Frenkel, E. Gazit, Phenylalanine assembly into toxic fibrils suggests amyloid etiology in phenylketonuria, Nat. Chem. Biol. 8 (8) (2012) 701.
[13] M. Taslimifar, S. Buoso, F. Verrey, V. Kurtcuoglu, Propagation of plasma L-phenylalanine concentration fluctuations to the neurovascular unit in phenylketonuria: an in silico study, Front. Physiol. 10 (2019) 360.
[14] T. Scarabino, T. Popolizio, M. Tosetti, D. Montanaro, G.M. Giannatempo, R. Terlizzi, S. Pollice, A. Maiorana, N. Maggialetti, A. Carriero, V. Leuzzi, U. Salvolini, Phenylketonuria: white-matter changes assessed by 3.0-T magnetic resonance (MR) imaging, MR spectroscopy and MR diffusion, Radiol. Med. 114 (2009) 461–474.
[15] V. Leuzzi, M. Tosetti, D. Montanaro, C. Carducci, C. Artiola, C. Carducci, I. Antonozzi, M. Burroni, F. Carnevale, F. Chiarotti, T. Popolizio, G. M. Giannatempo, V. D'Alesio, T. Scarabino, The pathogenesis of the white matter abnormalities in phenylketonuria. A multimodal 3.0 tesla MRI and magnetic resonance spectroscopy (1H MRS) study, J. Inherit. Metab. Dis. 30 (2007) 209–216.
[16] P.J. Anderson, V. Leuzzi, White matter pathology in phenylketonuria, Mol. Genet. Metab. 99 (2010) 3–9.
[17] J. Thompson, I. Smith, D. Brenton, B.D. Youl, G. Rylance, D.C. Davidson, B. Kendall, A.J. Lees, Neurological deterioration in young adults with phenylketonuria, Lancet 336 (1990) 602–605.
[18] P. Vermathen, L. Robert-Tissot, J. Pietz, T. Lutz, C. Boesch, R. Kreis, Characterization of white matter alterations in phenylketonuria by magnetic resonance relaxometry and diffusion tensor imaging, Magn. Reson. Med. 58 (2007) 1145–1156.
[19] R. Koch, S. Verma, F.H. Gilles, Neuropathology of a 4-month-old infant born to a woman with phenylketonuria, Dev. Med. Child Neurol. 50 (2008) 230–233.
[20] P. Morell, R.H. Quarles, The myelin sheath, in: G.J. Siegel, B.W. Agranoff, R. W. Albers, et al. (Eds.), Basic Neurochemistry: Molecular, Cellular And Medical Aspects, 6th edition, Lippincott-Raven, Philadelphia, 1999.
[21] M.A. Cleary, J.H. Walter, J.E. Wraith, F. White, K. Tyler, J.P. Jenkins, Magnetic resonance imaging in phenylketonuria: reversal of cerebral white matter change, J. Pediatr. 127 (1995) 251–255.
[22] C.A. Dyer, Pathophysiology of phenylketonuria, Ment. Retard. Dev. Disabil. Res. Rev. 5 (1999) 104–112.
[23] N. Joondan, P. Caumul, M. Akerman, S. Jhaumeer-Laulloo, Synthesis, micellisation and interaction of novel quaternary ammonium compounds derived from L-phenylalanine with 1,2-dipalmitoyl-snglycero-3-phosphocholine as model membrane in relation to their antibacterial activity, and their selectivity over human red blood cells, Bioorg. Chem. 58 (2015) 117–129.
[24] M. Shahmiri, Phenylalanine residues act as membrane anchors in the antimicrobial action of Aurein 1.2, Biointerphases 12 (2017) 05G605.
[25] T.D. Do, W.M. Kincannon, M.T. Bowers, Phenylalanine oligomers and fibrils: the mechanism of assembly and the importance of tetramers and counterions, J. Am. Chem. Soc. 137 (32) (2015) 10080.
[26] C. Poojaria, A. Kukolb, B. Strodel, How the amyloid-β peptide and membranes affect each other: an extensive simulation study, Biochim. Biophys. Acta Biomembr. 1828 (2) (2013) 327.
[27] C.M. Dobson, Protein folding and misfolding, Nature 426 (2003) 884.
[28] A.S. Rosa, A.C. Cutro, M.A. Frías, E.A. Disalvo, Interaction of phenylalanine with DPPC model membranes: more than a hydrophobic interaction, J. Phys. Chem. B 119 (52) (2015) 15844.
[29] K. Sankaranarayanan, Fibrils of phenylalanine adsorbed to Langmuir-Blodgett films: role of lipids, Soft Materials 13 (4) (2015) 219.
[30] E.C. Griffith, R.J. Perkins, D. Telesford, E.M. Adams, L. Cwiklik, H.C. Allen, M. Roeselová, V. Vaida, Interaction of L-phenylalanine with a phospholipid monolayer at thewater−air interface, J. Phys. Chem. B 119 (29) (2015) 9038.
[31] A.C. Cutró, A. Hollmann, J. Cejas, P. Maturana, E.A. Disalvo, M.A. Frías, Phenylalanine interaction with lipid monolayers at different pHs, Colloids Surf. B: Biointerfaces 135 (2015) 504.
[32] R. Perkins, V. Vaida, Phenylalanine increases membrane permeability, J. Am. Chem. Soc. 139 (2017) 14388–14391.
[33] L. Svennerholm, K. Bostrom, B. Jungbjer, L. Olsson, Membrane lipids of adult human brain: lipid composition of frontal and temporal lobe in subjects of age 20 to 100 years, J. Neurochem. 63 (1994) 1802–1811.
[34] M. Zoli, F. Benfenati, E.M. Pich, G. Toffano, K. Fuxe, L.F. Agnati, Aspects of neural plasticity in the central nervous system—IV. Chemical anatomical studies on the aging brain, Neurochem. Int. 16 (1990) 437–449.
[35] S. Hakomori, Carbohydrate–carbohydrate interaction as an initial step in cell recognition, Pure Appl. Chem. 63 (1991) 473–482.
[36] J.M. Boggs, A. Menikh, G. Rangaraj, Trans interactions between galactosylceramide and cerebroside sulfate across apposed bilayers, Biophys. J. 78 (2000) 874–885.
[37] J.M. Boggs, W. Gao, Y. Hirahara, Myelin glycosphingolipids, galactosylceramide and sulfatide, participate in carbohydrate–carbohydrate interactions between apposed membranes and may form glycosynapses between oligodendrocyte and/or myelin membranes, Biochim. Biophys. Acta Gen. Subj. 1780 (3) (2008) 445–455.
[38] J.M. Boggs, H. Wang, Effect of liposomes containing cerebroside and cerebroside sulfate on cytoskeleton of cultured oligodendrocytes, J. Neurosci. Res. 66 (2) (2001) 242–253.
[39] J. Zhao, Y. Liu, H. Park, J.M. Boggs, A. Basu, Carbohydrate-coated fluorescent silica nanoparticles as probes for the galactose/3-sulfogalactose carbohydrate−carbohydrate interaction using model systems and cellular binding studies, Bioconjug. Chem. 23 (2012) 1166–1173.
[40] J. Zhao, Y. Liu, H. Park, J.M. Boggs, A. Basu, Carbohydrate-coated fluorescent silica nanoparticles as probes for the galactose/3-sulfogalactose carbohydrate−carbohydrate interaction using model systems and cellular binding studies, Bioconjug. Chem. 23 (2012) 1166–1173.
[41] M. Aureli, L. Mauri, M.G. Ciampa, A. Prinetti, G. Toffano, C. Secchieri, S. Sonnino, GM1 ganglioside: past studies and future potential, Mol. Neurobiol. 53 (2016) 1824–1842.

[42] J.A. Krivanek, R.W. Ledeen, R.U. Margolis, R.K. Margolis, Gangliosides associated with microsomal subfractions of brain: comparison with synaptic plasma membranes, J. Neurobiol. 13 (1982) 95–106.
[43] R.W. Ledeen, Ganglioside structures and distribution: are they localized at the nerve ending? J. Supramol. Struct. 8 (1978) 1–17.
[44] R.W. Ledeen, G. Wu, New findings on nuclear gangliosides: overview on metabolism and function, J. Neurochem. 116 (2011) 714–720.
[45] C. Eggeling, C. Ringemann, R. Medda, B. Hein, S.W. Hell, High-resolution far-field fluorescence STED microscopy reveals nanoscale details of molecular membrane dynamics, Biophys. J. 96 (2009) 197a.
[46] C. Eggeling, C. Ringemann, R. Medda, G. Schwarzmann, K. Sandhoff, S. Polyakova, V.N. Belov, B. Hein, C. von Middendorff, A. Schonle, S.W. Hell, Direct observation of the nanoscale dynamics of membrane lipids in a living cell, Nature 457 (2009) 1159–1162.
[47] Akihiro Kusumi, Takahiro K. Fujiwara, Taka A. Tsunoyama, Rinshi S. Kasai, An-An Liu, Koichiro M. Hirosawa, Masanao Kinoshita, Nobuaki Matsumori, Naoko Komura, Hiromune Ando, Kenichi G.N. Suzuki, Defining raft domains in the plasma membrane, Traffic 21 (2020) 106–137.
[48] K. Simons, E. Ikonen, Functional rafts in cell membranes, Nature 387 (1997) 569–572.
[49] M. Piccinini, F. Scandroglio, S. Prioni, B. Buccinna, N. Loberto, M. Aureli, V. Chigorno, E. Lupino, G. DeMarco, A. Lomartire, M.T. Rinaudo, S. Sonnino, A. Prinetti, Deregulated sphingolipid metabolism and membrane organization in neurodegenerative disorders, Mol. Neurobiol. 41 (2010) 314–340.
[50] J.E. Vance, Dysregulation of cholesterol balance in the brain: contribution to neurodegenerative diseases, Dis. Model. Mech. 5 (2012) 746–755.
[51] S. Sonnino, M. Aureli, S. Grassi, L. Mauri, S. Prioni, A. Prinetti, Lipid rafts in neurodegeneration and neuroprotection, Mol. Neurobiol. 50 (1) (2013) 130–148.
[52] K.L. Hudson, G.J. Bartlett, R.C. Diehl, J. Agirre, T. Gallagher, L.L. Kiessling, D. N. Woolfson, Carbohydrate−aromatic interactions in proteins, J. Am. Chem. Soc. 137 (2015) 15152–15160.
[53] A. De Luigi, A. Mariani, M. De Paola, Depaolini A. Re, L. Colombo, L. Russo, V. Rondelli, P. Brocca, L. Adler-Abramovich, E. Gazit, E. Del Favero, L. Cantù, M. Salmona, Doxycycline hinders phenylalanine fibril assemblies revealing a potential novel therapeutic approach in phenylketonuria, Sci. Rep. 5 (2015) 15902.
[54] S. Haik, et al., Doxycycline in Creutzfeldt-Jakob disease: a phase 2, randomised, double-blind, placebo-controlled trial, Lancet Neurol. 13 (2) (2014) 150.
[55] P. Adamczewski, V. Tsoukanova, Phenylalanine intercalation parameters for liquid-disordered phase domains – a membrane model study, BMC, Biophysics 11 (6) (2018).
[56] R.A. Reed, G.G. Shipley, Properties of ganglioside GM1 in phosphatidylcholine bilayer membranes, Biophys. J. 70 (1996) 1363–1372.
[57] V. Rondelli, E. Del Favero, S. Motta, et al., Neutrons for rafts, rafts for neutrons, Eur. Phys. J. E 36 (2013) 73.
[58] V. Rondelli, G. Fragneto, S. Motta, E. Del Favero, P. Brocca, S. Sonnino, L. Cantù, Ganglioside GM1 forces the redistribution of cholesterol in a biomimetic membrane, Biochim. Biophys. Acta Biomembr. 1818 (11) (2012) 2860–2867.
[59] D. Marquardt, F.A. Heberle, J.D. Nickels, G. Pabst, J. Katsaras, On scattered waves and lipid domains: detecting membrane rafts with X-rays and neutrons, Soft Matter 11 (2015) 9055–9220.
[60] V. Rondelli, P. Brocca, S. Motta, M. Messa, L. Colombo, M. Salmona, G. Fragneto, L. Cantù, E. Del Favero, Amyloid-β peptides in interaction with raft-mime model membranes: a neutron reflectivity insight, Sci. Rep. 6 (2016) 20997.
[61] F. Perissinotto, V. Rondelli, P. Parisse, N. Tormena, A. Zunino, L. Almásy, D. G. Merkel, L. Bottyán, S.z. Sajti, L. Casalis, GM1 Ganglioside role in the interaction of Alpha-synuclein with lipid membranes: Morphology and structure, Biophys. Chem. 255 (2019), 106272.
[62] V. Rondelli, M. Salmona, L. Colombo, G. Fragneto, G.C. Fadda, L. Cantu', E. Del Favero, Aβ beyond the AD pathology: exploring the structural response of membranes exposed to nascent Aβ peptide, Int. J. Mol. Sci. 21 (2020) 8295.
[63] F. Perissinotto, V. Rondelli, B. Senigagliesi, P. Brocca, L. Almásy, L. Bottyán, D. Géza Merkel, H. Amenitsch, B. Sartori, K. Pachler, M. Mayr, M. Gimona, E. Rohde, L. Casalis, P. Parisse, Structural insights into fusion mechanisms of small extracellular vesicles with model plasma membranes, Nanoscale 13 (2021) 5224–5233.
[64] Sourav Nandi, Arghajit Pyne, Meghna Ghosh, Pavel Banerjee, Biswajoy Ghosh, Nilmoni Sarkar, Antagonist effects of l-phenylalanine and the enantiomeric mixture containing d-phenylalanine on phospholipid vesicle membrane, Langmuir 36 (9) (2020) 2459–2473.
[65] V. Engelbrecht, A. Scherer, M. Rassek, H.J. Witsack, U. Modder, Diffusion weighted MR imaging in the brain in children: findings in the normal brain and in the brain with white matter diseases, Radiology 222 (2002) 410–418.
[66] J. Takanashi, K. Hirasawa, H. Tada, Reversible restricted diffusion of entire corpus callosum, J. Neurol. Sci. 247 (2006) 101–104.
[67] T.J. Buscham, M.A. Eichel, S.B. Siems, H.B. Werner, Turning to myelin turnover, Neural Regen. Res. 14 (12) (2019) 2063–2066.
[68] O. Jahn, S. Tenzer, B. WernerH, Myelin proteomics: molecular anatomyof an insulating sheath, Mol. Neurobiol. 40 (2009) 55–72.
[69] G. Forloni, L. Colombo, L. Girola, F. Tagliavini, M. Salmona, Anti-amyloidogenic activity of tetracyclines: studies in vitro, FEBS Lett. 487 (3) (2001) 404–407.
[70] Fabrizio Tagliavini, Gianluigi Forloni, Laura Colombo, Giacomina Rossi, Laura Girola, Barbara Canciani, Nadia Angeretti, Lidia Giampaolo, Elisa Peressini, Tazeen Awan, Luca De Gioia, Enzio Ragg, Orso Bugiani, Mario Salmona, Tetracycline affects abnormal properties of synthetic PrP peptides and PrPSc in vitro, J. Mol. Biol. 300 (5) (2000) 1309–1322.
[71] T. Stoilova, L. Colombo, G. Forloni, F. Tagliavini, M. Salmona, A new face for old antibiotics: tetracyclines in treatment of amyloidoses, J. Med. Chem. 56 (15) (2013 Aug 8) 5987–6006.